F

Internal Report
DESY D3-86
January 1997

Sight cuts

Production of radioactive nuclides in soil and groundwater near the beam dump of a Linear Collider

K. Tesch

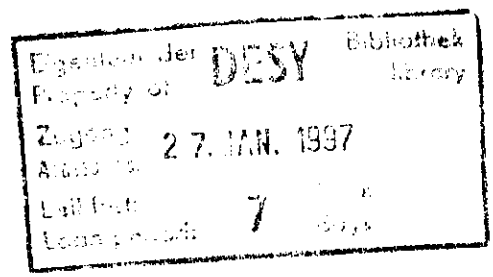

Internal Report
DESY D3-86
January 1997

Production of radioactive nuclides in soil and groundwater near the beam dump of a Linear Collider

K. Tesch

Abstract: Activities of accelerator-produced nuclei near the tunnel of an electron-positron linear collider are calculated. The method makes use of (a) a calculated spectrum of neutrons produced in the beam dump, (b) approximated neutron cross sections, (c) assumptions on the mean beam power averaged over long time periods. The final numerical results are preliminary.

1. Introduction

It has been proposed in a Conceptional Design Report [1] to build a Linear Collider in which an electron beam and a positron beam are accelerated against each other. Both beams have an energy of 250 GeV, the number of particles/s is $2 \cdot 10^{14}$ giving a mean beam power of 8 MW. The beams (or about 85 % of them) are dumped into absorbers after having passed the interaction point and some beamstrahlung collimators. Only materials like carbon or water can withstand such high mean powers. In the following we assume the carbon dump proposed to avoid the strong hydrolysis of water and the handling of liquid radioactive waste. Fig. 1A shows a possible scheme of a dump with a graphite core and backing aluminium together with a beam sweeping system to enlarge the extremly thin beam cross section and to distribute it along the front face (from [1]). Additional lead shields may be necessary to reduce the dose rate due to residual radioactivity, depending on the position of the dump.

The tunnel for the two linacs is constructed deep underground, its place is mainly in the district Kreis Pinneberg north-west of DESY. The thickness of soil above tunnel varies between 7 m (when crossing two small brooks) and 15 m for a possible tunnel position; the tunnel dives into ground water.

The proposed dump is large enough to absorb more than 95 % of the beam energy. This means that any production of radioactive nuclei outside the dump and outside the tunnel is caused by medium-energy and low-energy neutrons escaping the dump and by high-energy particles in the forward direction (whereas the very high activation of the dump itself is mainly due to the photons of the electromagnetic cascade). In order to calculate this production in soil and in ground water near the dump only the neutrons are considered. For this the knowledge of the neutron spectrum and of the nuclear cross sections are necessary. The information on both subjects are collected in the two following sections. The results in sections 4 and 5 are included in the report [1].

The intention of this report is to demonstrate the method by which activities of accelerator-produced nuclides are calculated. The final results are very

preliminary. At least two improvements will be necessary: a better calculation of the neutron spectrum with the most recent Monte Carlo code and for the actual dump geometry, and better information on the groundwater near the tunnel, its movement and its use, by means of a hydrological expertise.

2. The neutron spectrum

The spectrum of neutrons produced by high energy protons in a thick target is well known both from experiments and from calculations. Unfortunately no measurements on neutron spectra produced by high energy electrons are known to verify calculations. Such calculations can be done by means of a Monte Carlo code for primary electrons which was developed very recently [2]. We used the earlier version FLUKA 92 for the present. The calculated spectra of neutrons produced in a thick iron target and behind a concrete side shield turned out to resemble the known neutron spectra produced by primary protons in the same shielding geometry. Also the neutron dose equivalent attenuation coefficients are not too different for both cases [3, 4]. This similarity can be expected. Neutrons in the relevant range up to 200 MeV and at large angles are produced by intranuclear cascades (initiated by particles below 0.5-1 GeV) and by low energy nuclear reactions in a thick target and in the concrete or sand shield rather independent of the high energy processes. Important for the present problem is the large portion of high energy neutrons $(E_n > 20\ \mathrm{MeV})$ in the spectrum. In this energy range neutron cross sections are known only rather inaccurately or are missing (see next section). As a consequence, the accuracy of calculations of nuclear processes outside the tunnel is not determined by inadequate knowledge on neutron spectra but by the available information on cross sections. Therefore we used our preliminary calculations for an iron dump and concrete side shielding (instead of a C/Al dump + heavy metal shield and concrete/sand side shielding); the resulting neutron spectrum being independent of shield thicknesses larger than 60 cm was normalized in such a way that its dose equivalent gives the dose values of [3] for an aluminium dump, they in turn are a summary of earlier experimental and theoretical results. The resulting fluence spectrum per one incident 100–GeV

electron, behind a side shield of 200 g/cm^2 concrete or sand and at a distance of 3 m from target, is given in tab. 1.

Tab. 1.

E (MeV)	ϕ d E$*10^9$ (cm^{-2})
1.1-1.3	4.2
1.3-1.6	4.6
1.6-2.0	5.1
2.0-2.5	7.6
2.5-3.0	6.6
3.0-3.7	4.4
3.7-4.5	4.4
4.5-5.5	4.2
5.5-6.7	4.5
6.7-8.2	3.8
8.2-10	3.3
10-12	3.3
12-13	2.3
13-15	2.8
15-17	2.6
17-20	2.6
20-37	22
37-68	38
67-125	48
125-230	34
230-420	11
420-720	1.7
780-1400	0.08
$1\cdot10^{-10}$-$1\cdot20^{-6}$	7.8

3. Reaction cross sections

The relevant components of soil and of ground water are indicated in tab. 2; the dissolved constituents of water are from an analysis of ground water at DESY.

Tab. 2.

Element	Percentage by weight soil	water	Nuclear reaction
O	53	89	^{16}O (n, 2 α 2 n) ^{7}Be; ^{16}O (n, x) ^{3}H
Si	32		^{28}Si (n, x) ^{7}Be; ^{28}Si (n, x) ^{3}H; ^{28}Si (n, α p 2 n) ^{22}Na
Al	4		^{27}Al (n, α 2 n) ^{22}Na
Ca	3	$5 \cdot 10^{-3}$	^{44}Ca (n, γ) ^{45}Ca
Mg	2	$1.5 \cdot 10^{-3}$	^{24}Mg (n, p 2 n) ^{22}Na
Fe	2	$1 \cdot 10^{-4}$	^{54}Fe (n, p) ^{54}Mn; ^{56}Fe (n, 2 n) ^{55}Fe
C	1	$8 \cdot 10^{-4}$	----------
Na	1	$3 \cdot 10^{-3}$	^{23}Na (n, 2 n) ^{22}Na
K	1		----------
Mn	0.5	$5 \cdot 10^{-5}$	^{55}Mn (n, 2 n) ^{54}Mn
Cl		$7 \cdot 10^{-3}$	----------
S		$3 \cdot 10^{-3}$	----------
P		$2 \cdot 10^{-6}$	----------

Only radioactive nuclides with half lifes between 30 d and 100 a are considered, the producing reactions are also entered into the table. All such reactions are important for the target nuclei oxygen and silicon because of the high abundance of these elements. For the other elements only simple reactions are considered and especially no spallation reactions producing ^{3}H and ^{7}Be because the cross sections are too small. Cross sections are known only for some of them in the energy range up to 20 MeV, whereas the neutron spectrum extends up to 300 MeV. In most cases approximations were necessary: substitution of neutron cross sections by those for a known proton-induced reaction giving the same nuclide, extrapolations to higher energies, interpolation between different measured values. The details are given in the following for each reaction. The hatched curves in the figures are the approximations used in the calculations. The difference between the characteristic shapes of spallation reactions and of simple reactions is apparent.

^{16}O (n, 2 α 2 n) ^{7}Be.

Q = – 33.4 MeV. Also ^{16}O (n, α 2 p 4 n) ^{7}Be, Q = – 62 MeV, and ^{16}O (n, 4 p 6 n) ^{7}Be, Q = – 90 MeV. Cross sections unknown, substituted by ^{16}O (p, 2 α p n) ^{7}Be, Q = – 33.4 MeV. Fig. 1.

^{16}O (n, x) ^{3}H.

Q = – 14.4 MeV. Cross sections unknown, substituted by ^{16}O (p, x) ^{3}H, Q = – 20 MeV. Fig. 2. Comparison with ^{27}Al (n, x) ^{3}H.

^{28}Si (n, x) ^{7}Be.

Cross sections unknown, substituted by ^{28}Si (p, x) ^{7}Be. Fig. 3.

^{28}Si (n, x) ^{3}H

Q = – 16.1 MeV. Cross sections unknown, substituted by ^{28}Si (p, x) ^{3}H. Curve similar to ^{16}O (p, x) ^{3}H and ^{28}Si (p, x) ^{7}Be. Fig. 4.

^{28}Si (n, α p 2 n) ^{22}Na

Q = – 26.5 MeV. Also ^{28}Si (n, 3 p 4 n) ^{22}Na, Q = – 62 MeV.
Cross sections unknown, substituted by ^{28}Si (p, α 2 p n) ^{22}Na, Q = – 34 MeV. Fig. 5.

^{23}Na (n, 2 n) ^{22}Na

Q = – 12.4 MeV. Cross sections not in agreement, comparison also with ^{23}Na (p, p n) ^{22}Na, Q = – 13 MeV. Fig. 6.

^{27}Al (n, α 2 n) ^{22}Na

Q = – 22.5 MeV. Also ^{27}Al (n, 2 p 4 n) ^{22}Na, Q = – 50.8 MeV. Cross sections unknown, substituted by ^{27}Al (p, α p n) ^{22}Na, Q = – 22.5 MeV. Fig. 7.

^{55}Mn (n, 2 n) ^{54}Mn

Fig. 8. Extrapolated in comparison with ^{55}Mn (p, p n) ^{54}Mn

^{54}Fe (n, p) ^{54}Mn. Fig. 9.

^{56}Fe (n, 2 n) ^{55}Fe

Fig. 10. Comparison with ^{56}Fe (p,p n) ^{55}Fe.

^{24}Mg (n, p 2 n) ^{22}Na

Cross sections unknown, substituted by ^{24}Mg (p, 2 p n) ^{22}Na. Fig. 11.

4. Accelerator-produced nuclei in soil

The saturation activity of produced nuclei is calculated by

$$A_S = n \int \sigma(E)\ \phi(E)\, dE,$$

A_S is the saturation activity concentration in Bq/g, n is the number of target nuclei per gram, σ the nuclear cross section in cm^2, $\phi\, dE$ the neutron flux density (cm^{-2} s^{-1}) in the energy intervall d E. The necessary data are given in the preceding sections; A_S values of soil near the beam dump (about 0.5 m distant from the concrete tunnel) are presented in tab. 3 per one 100–GeV electron/s.

Tab. 3.

Reaction	Half life	n (g^{-1})	A_S (Bq/g) per 100–GeV e/s
^{16}O (n, 2α 2n) ^{7}Be	53 d	2.0 +22	1.2–11
^{16}O (n, x) ^{3}H	12.3 a		3.6–11
^{28}Si (n, x) ^{7}Be	53 d	6.9+21	8.3–13
^{28}Si (n, x) ^{3}H	12.3 a		9.7–12
^{28}Si (n, α p 2n) ^{22}Na	2.6 a		1.6–11
^{23}Na (n, 2n) ^{22}Na		2.6+20	2.0–12
^{27}Al (n, α 2n) ^{22}Na		8.9+20	2.9–12
^{24}Mg (n, p 2n) ^{22}Na		3.9+20	2.5–12
^{55}Mn (n, 2n) ^{54}Mn	310 d	5.5+19	3.5–14
^{54}Fe (n, p) ^{54}Mn		1.3+19	2.7–13
^{56}Fe (n, 2n) ^{55}Fe	2.7 a	2.0+20	5.8–12
^{44}Ca (n, γ) ^{45}Ca	160 d	8.6+18	5.9–13

Some of the resulting activities are changed due to the moving groundwater which is discussed in the next section. Here we only note that the produced ^{3}H is dissolved in and transported by the water, it does not add to the total soil activity. The small soluble fraction of ^{22}Na can be neglected.

In order to calculate the saturation activities produced by the operation of the linac one has to assume a mean beam power averaged over a time period which equals about twice the half life of the nuclide. The assumed mean power values are in tab. 4.

Tab. 4.

Time period	$\bar{p}$ (MW)
1 h	8
100 d	2
1 a	1
5 a	0.5
25 a	0.5

We receive the saturation activity concentrations of the 5 relevant nuclides near the beam dump by means of tab. 3 and 4, they are given in tab. 5.

Tab. 5.

Nuclide	Half life	$\bar{p}$ (MW)	A_S (Bq/g)
^{7}Be	53 d	2	1600
^{22}Na	2.6 a	0.5	730
^{45}Ca	160 d	1	36
^{54}Mn	310 d	1	19
^{55}Fe	2.7 a	0.5	180

The summed total activity of all 5 nuclides depends on the linac operation as a function of time, only in the most unfavourable case it is the sum of the values of tab. 5. It can be a factor of 1000 higher than, e. g., the natural ^{40}K activity of sand, but apparently it presents no radiological problem: The nuclides are permanently attached to solid soil and are neither accessible nor movable; the amount of soil with the indicated activities is less than 300 m^3; all half lifes are smaller than

3 years, 30 years after a final shutdown of the accelerator the activities are below the natural activity of sand. If necessary, the activities produced in soil can be reduced by additional concrete surrounding the tunnel near to the beam dump which is also discussed in the section 5. The calculated activities cannot be compared with maximum permissible activity concentrations since such limits are not given in most national radiation protection regulations (e. g. in Germany, Switzerland, or Japan).

5. Accelerator-produced nuclides in groundwater

The components of groundwater and possible reactions were already given in tab. 2. The activity concentrations at saturation are calculated in the same way as in section 4, tab. 6 shows the results per one 100–GeV electron/s.

Tab. 6.

Reaction	n (g^{-1})	A_S (Bq/g) per 100–GeV e/s
^{16}O (n, 2α 2n) ^{7}Be	3.3+22	2.0–11
^{16}O (n, x) ^{3}H		5.9–11
^{23}Na (n, 2n) ^{22}Na	7.9+17	5.9–15
^{55}Mn (n, 2n) ^{54}Mn	5.0+15	3.2–18
^{54}Fe (n, p) ^{54}Mn	6.5+14	1.4–17
^{56}Fe (n, 2n) ^{55}Fe	9.9+15	2.9–16
^{44}Ca (n, γ) ^{45}Ca	1.4+16	9.7–16

Reactions with dissolved nuclei are apparently negligible and will be neglected in the following. More important is the effect of water on nuclides produced in soil and of the movement of groundwater, in addition to spallation of oxygen. These effects are rather complicated, from the literature we have the following information.

^{3}H: all tritium produced in soil or water is dissolved in water and will be transported with the velocity of the water [22].

^{7}Be: is very strongly absorbed, 100 % in resin beds [23]; a strong chemical affinity is reported for soil [24] and 100 % absorption in chalk [25].

^{22}Na: 15 % of the produced nuclei is soluble, a small part (2 %) of it is absorbed again in other soil layers; the other 85 % are nearly insoluble when produced in sand, silt, or clay (glacial till) [22]. Others report a solubility of 15 % [26] or 10 % [24].

^{45}Ca: a small fraction (< 5 %) is soluble [22].

^{54}Mn: weakly soluble, depending on kind of soil [24]. Solubility (< 5 %) [26].

From these results and from tabs. 5 and 6 we conclude that for a discussion of groundwater contamination we can neglect the nuclides ^{7}Be, ^{45}Ca, and ^{54}Mn; we also neglect ^{55}Fe though we have no information on its chemical behaviour, but its contribution is low anyway. Radioactive nuclei in groundwater are mainly ^{3}H and ^{22}Na; this conclusion has recently been confirmed by experiment [24].

In order to calculate the activity concentrations of these two nuclides in the groundwater near to the beam dump, we assume a rest time (= irradiation time) of the water near to the tunnel of 100 d (as long as we have no better hydrological information). The resulting concentrations will be compared with maximum permissible concentrations for the yearly water consumption of a person, therefore we assume a mean beam power averaged over one year which is 1 MW (tab. 4). The water content of soil below the ground water level is 28 % at the DESY site, its density about 2 g/cm^{3}. We assume that all ^{3}H produced in soil is leached by the water and adds to the ^{3}H produced by spallation in water; 15 % of ^{22}Na produced in soil by different nuclear reactions is dissolved. Then we receive from tabs. 5 and 6 the activity concentrations 180 Bq/g for ^{3}H and 40 Bq/g for ^{22}Na near to the tunnel where the main beam dump is positioned.

These numbers can be compared with concentrations in drinking water. According to the German Radiation Protection Regulation activity concentrations of 22 Bq/g and 0.060 Bq/g for ^{3}H and ^{22}Na, respectively, will result in an effective dose of 0.3 mSv/a (for a consumption of 0.8 m^3 per year) which is the maximum permissible dose for the general public. These concentrations are received with a dilution of about 1:500 which is easily achieved since our results refer to roughly 100 m^3 water,a very small amount compared with the huge reservoir within a water table.

If, however, private wells are in use in the neighbourhood of the tunnel additional precautions can be taken. Neutron fluxes can by reduced by additional concrete. A reduction by a factor of 30 is achieved by shielding the dump inside the tunnel with 1m heavy concrete (ρ = 3.7 g/cm^3). Another possibility is to seperate the water near the tunnel from the moving groundwater by means of cutoff walls or plastic foils, a technique which is occasionally in use near a disposal of chemical waste.

6. References

1. Conceptual Design Report, DESY 1997.
2. A. Fassò, A. Ferrari, P. R. Sala, 8th. Intern. Conf. Radiation Shielding, Arlington 1994
3. K. Tesch, Rad. Prot. Dosimetry 22 (1988) 27
4. A. Fassò, M. Höfert, A. Ioannidou, Rad. Prot. Dosimetry 38 (1991) 301
5. H. W. Bertini et al., ORNL - 3884 (1966)
6. R. Silberberg, C. H. Tsao, Naval Research Lab., NRL 7593 (1973)
7. Landolt-Börnstein, Numerical Data in Science and Technology NS, Vol. 1.5 b, Springer Verlag
8. S. T. Kruger, D. Heymann, Phys. Rev. C7 (1973) 2179
9. V. Mc Lane, C. L. Dunford, P. Rose, Neutron cross sections, Vol. 2, Academic Press 1988
10. G. M. Raisbeck, F. Yion, Phys. Rev. C12 (1975) 915
11. H. R. Heydegger et al., Phys. Rev. C14 (1976) 1506
12. D. I. Garber, R.R. Kinsey, Neutron cross sections, 3rd. edition, Vol. II, BNL 325, 1976
13. Y. Uwamino et al., Nucl. Sei. Eng. 111 (1992) 391

14. M. Gusakov, Ann. Phys. 7 (1962) 67
15. R. Korteling, A. A. Caretto, Phys. Rev. C1 (1970) 1960
16. P. Benioff, Phys. Rev. 119 (1960) 316
17. E. Bruninx, CERN 64-17 (1964)
18. N. M. Hintz, N. F. Ramsey, Phys. Rev. 88 (1952) 19
19. C. B. Cumming, Ann. Rev. Nucl. Sci 13 (1963)
20. J. E. Cline, E. B. Nieschmidt, Nucl. Phys. A 169 (1971) 437
21. K. Miyano, J. Phys. Soc. Japan 34 (1973) 853
22. T. B. Borak et al., Health Phys. 23 (1972) 679
23. A. Rindi, CERN Lab. II - RA / Note/ 72-23 (1972)
24. S. Baker, J. Bull, D. Goss, SSC Dallas, SSCL-Preprint 538 (1994)
25. R. H. Thomas, KEK-78-20 (1978)
26. A. A. Aleksadrov et al., Sov. At. Energy 34 (1973) 227

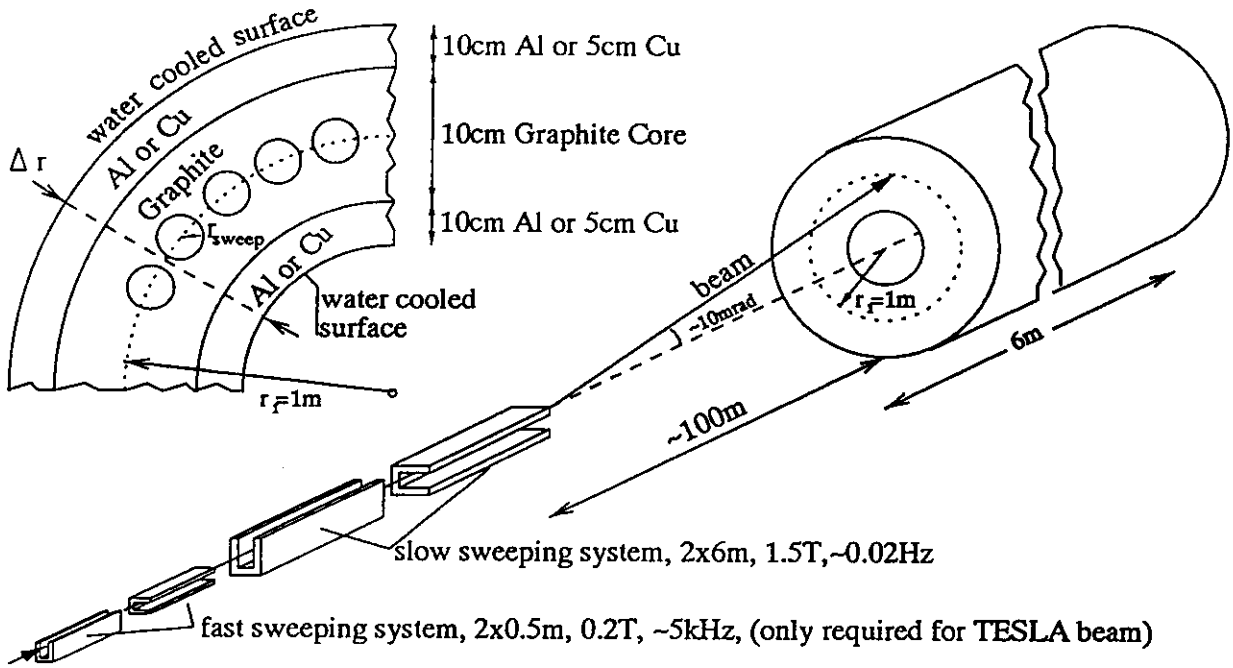
water cooled surface
Δ r
Al or Cu
Graphite
r sweep
Al or Cu
10cm Al or 5cm Cu
10cm Graphite Core
10cm Al or 5cm Cu
water cooled surface
r f=1m
beam
~10mrad
r f=1m
6m
~100m
slow sweeping system, 2x6m, 1.5T,~0.02Hz
fast sweeping system, 2x0.5m, 0.2T, ~5kHz, (only required for TESLA beam)
particle beam of 250GeV

Fig. 1A

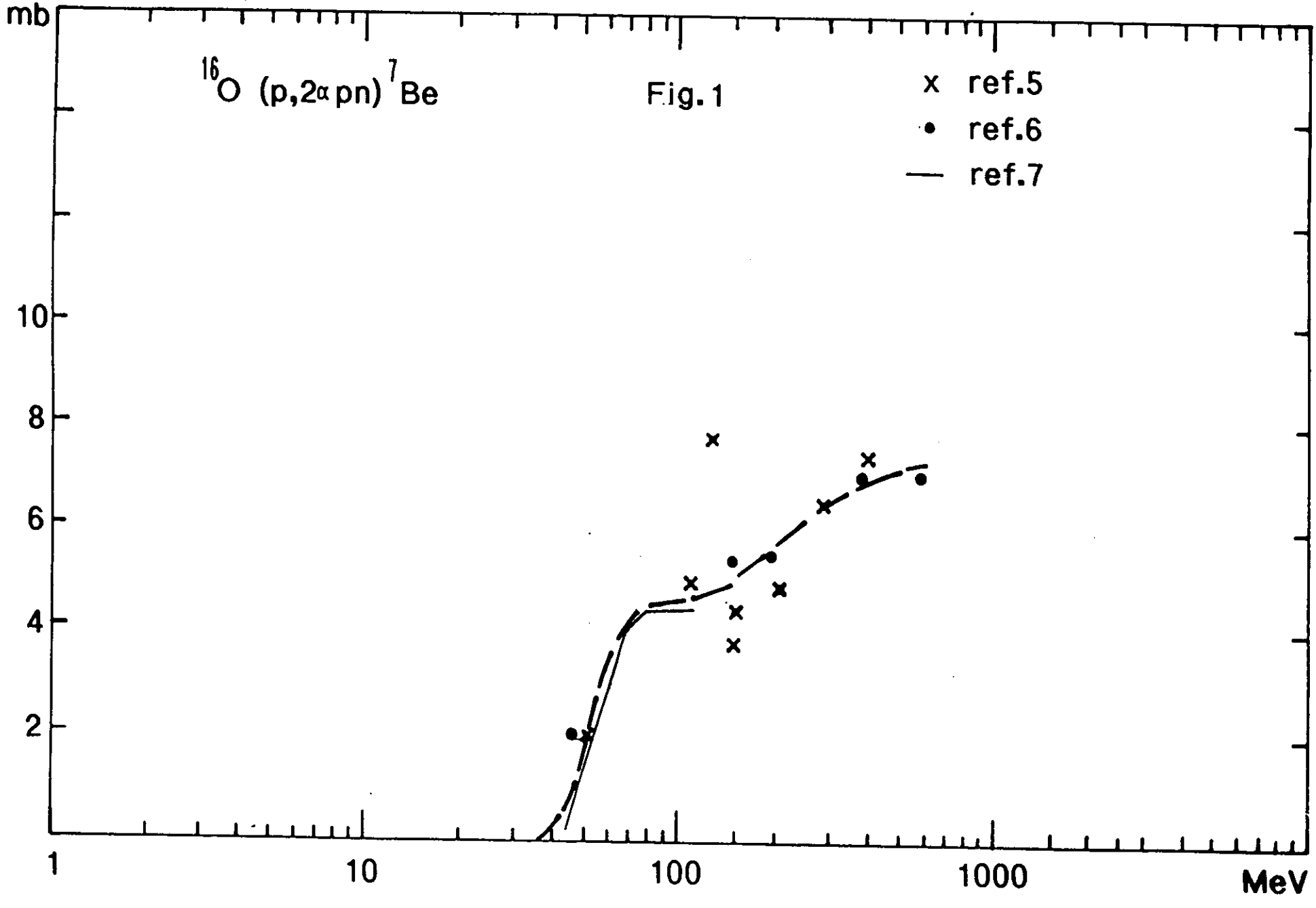
mb
^{16}O (p,2α pn) ^{7}Be
Fig. 1
x ref.5
• ref.6
— ref.7
10
8
6
4
2
1
10
100
1000
MeV

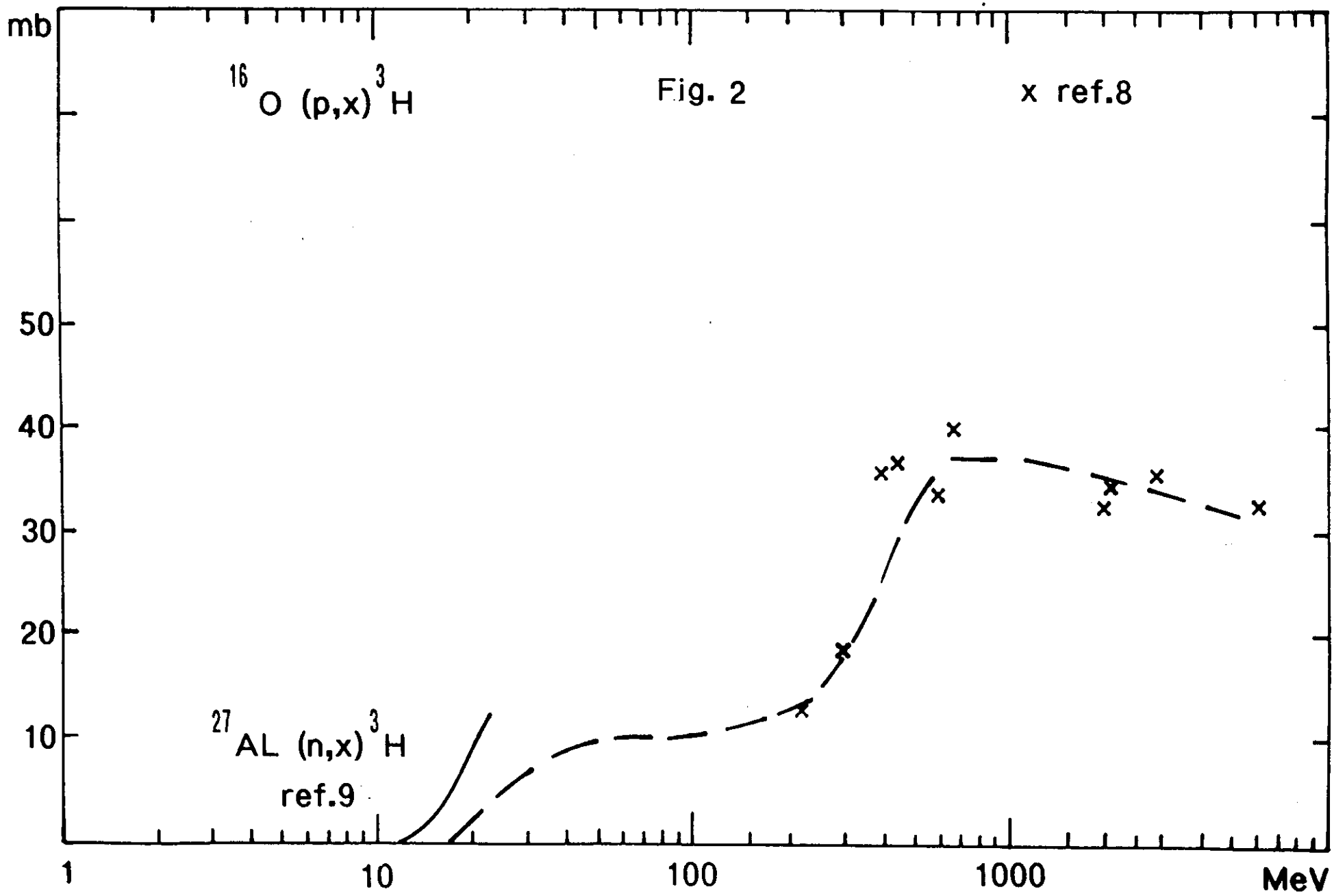
mb
^{16}O (p,x)^{3}H
Fig. 2
x ref.8
50
40
30
20
10
^{27}AL (n,x)^{3}H
ref.9
1
10
100
1000
MeV

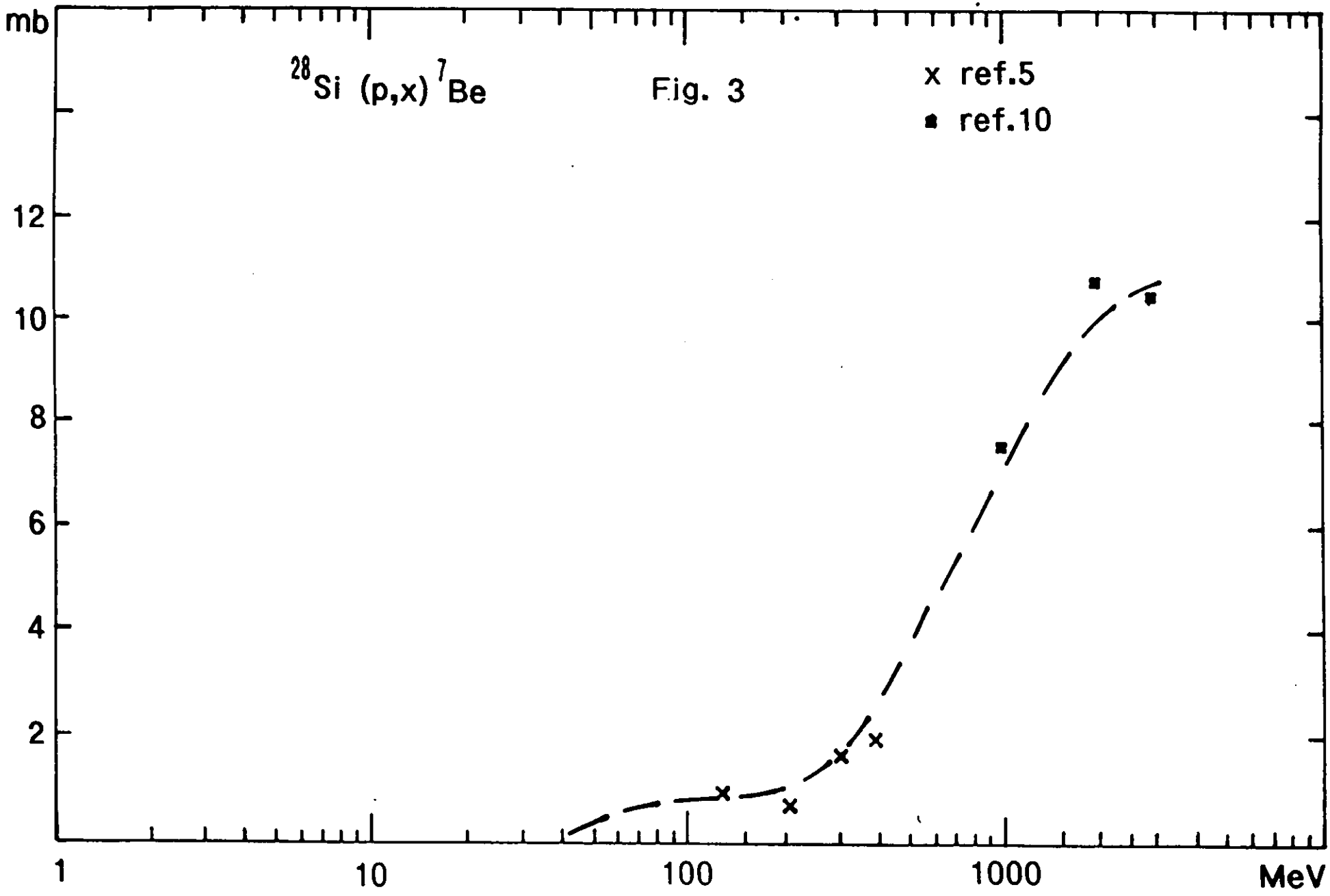
mb
^{28}Si (p,x) ^{7}Be
Fig. 3
x ref.5
ref.10
12
10
8
6
4
2
1
10
100
1000
MeV

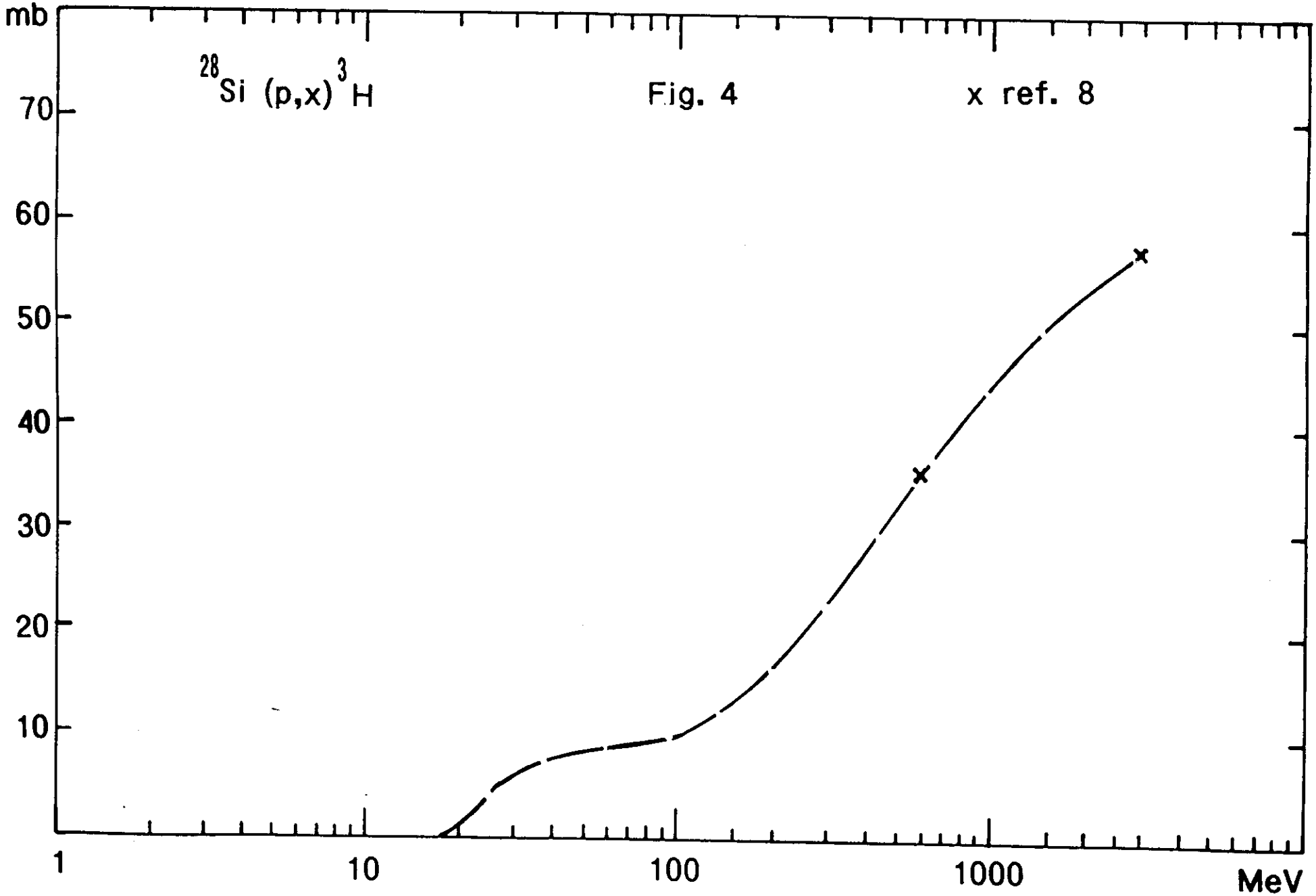
mb
^{28}Si (p,x)^{3}H
Fig. 4
x ref. 8
70
60
50
40
30
20
10
1
10
100
1000
MeV

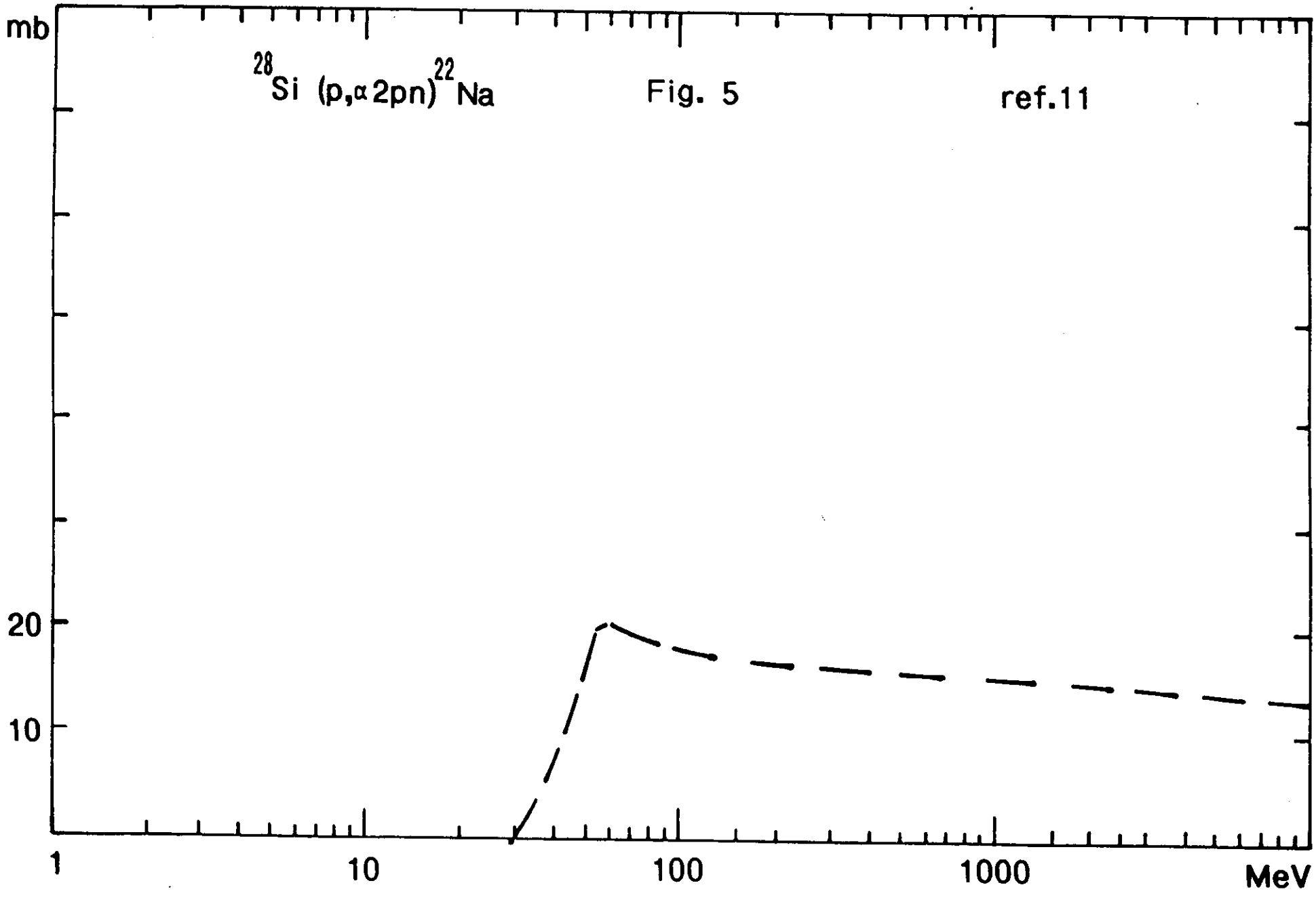
mb
^{28}Si (p,α2pn)^{22}Na
Fig. 5
ref.11
20
10
1
10
100
1000
MeV

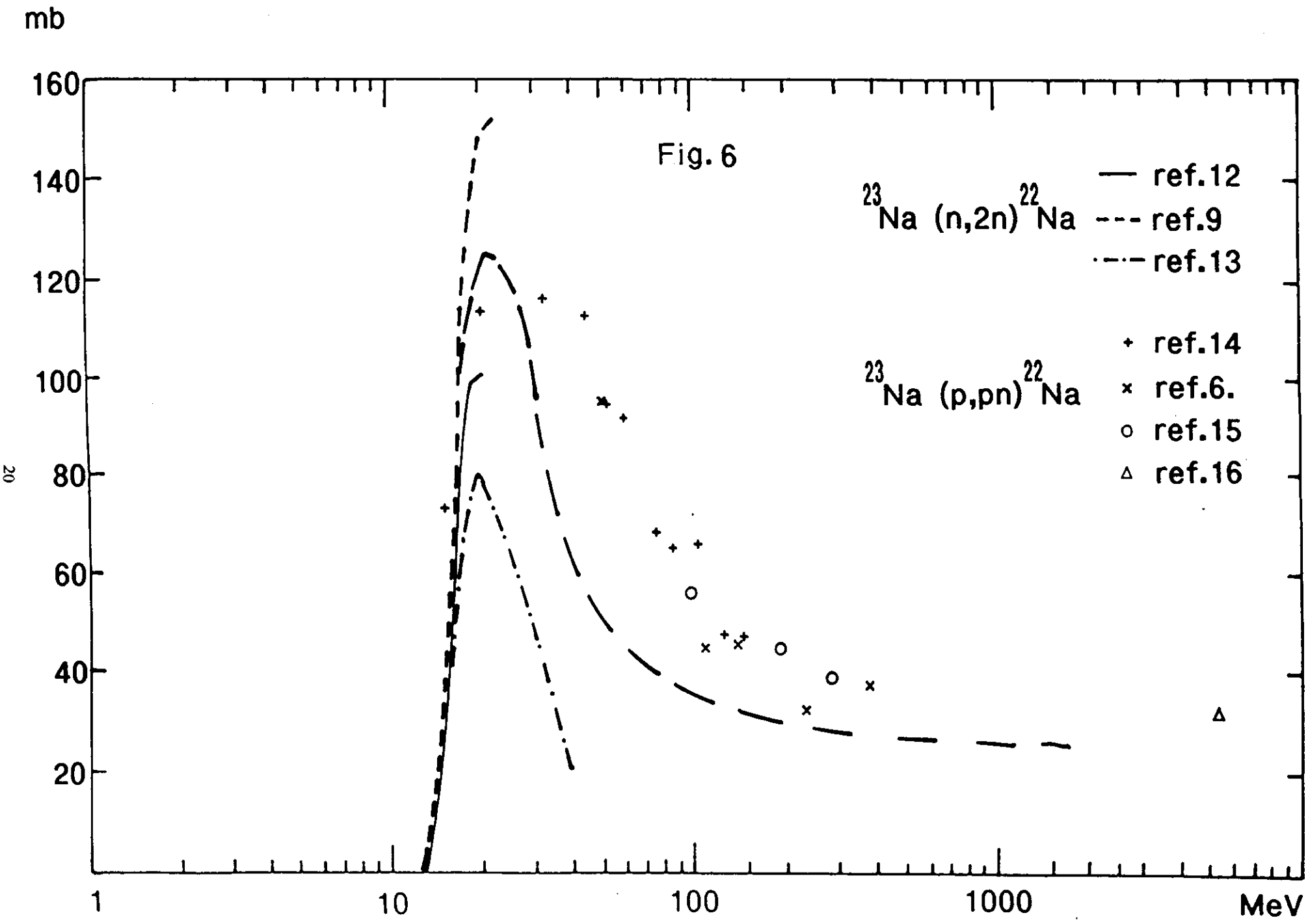
mb
160
140
120
100
80
60
40
20
1
10
100
1000
MeV
Fig. 6
23Na (n,2n) 22Na
ref.12
ref.9
ref.13
23Na (p,pn) 22Na
ref.14
ref.6.
ref.15
ref.16

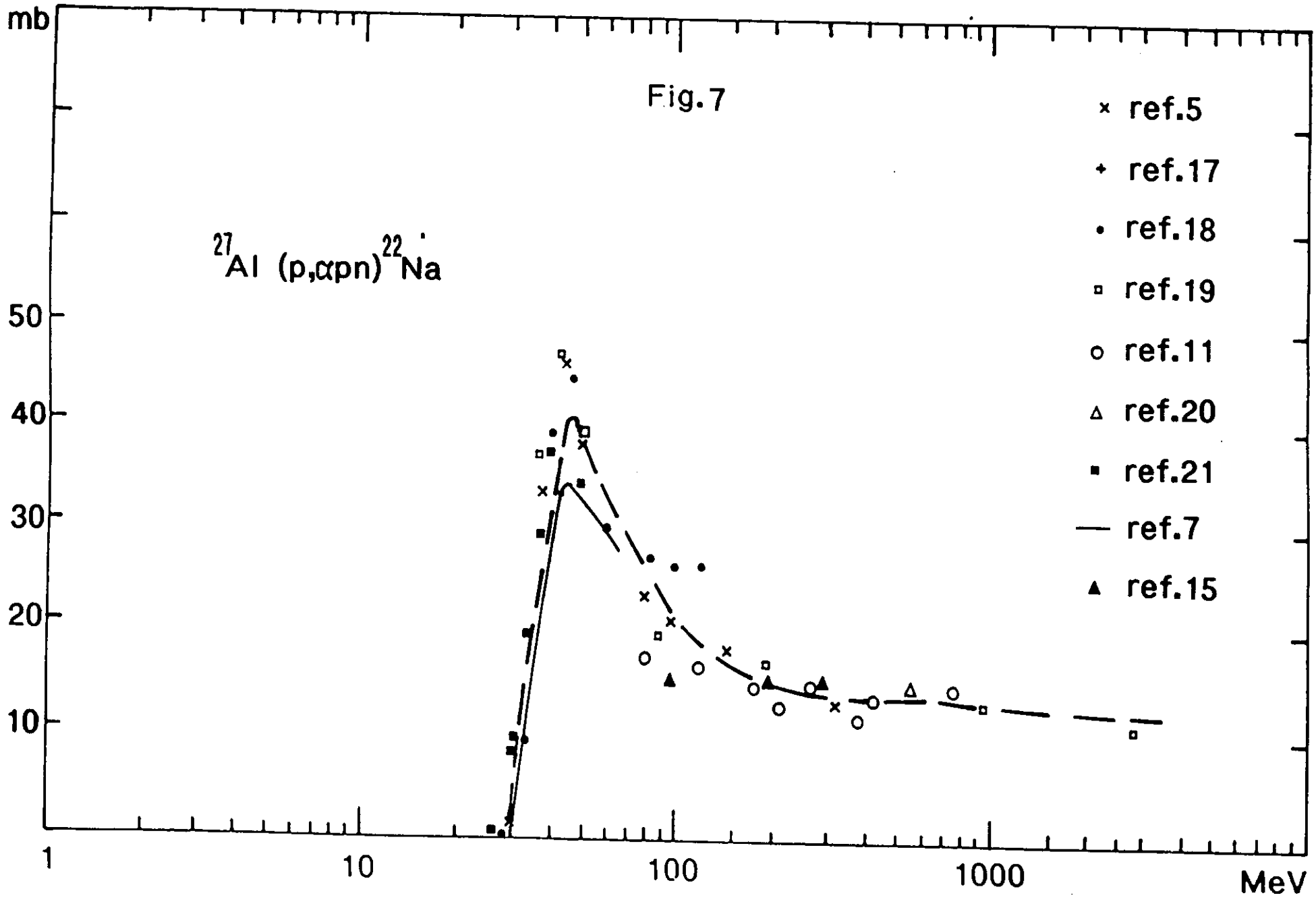
mb
Fig.7
$^{27}Al\ (p,\alpha pn)^{22}Na$
ref.5
ref.17
ref.18
ref.19
ref.11
ref.20
ref.21
ref.7
ref.15
50
40
30
20
10
1
10
100
1000
MeV

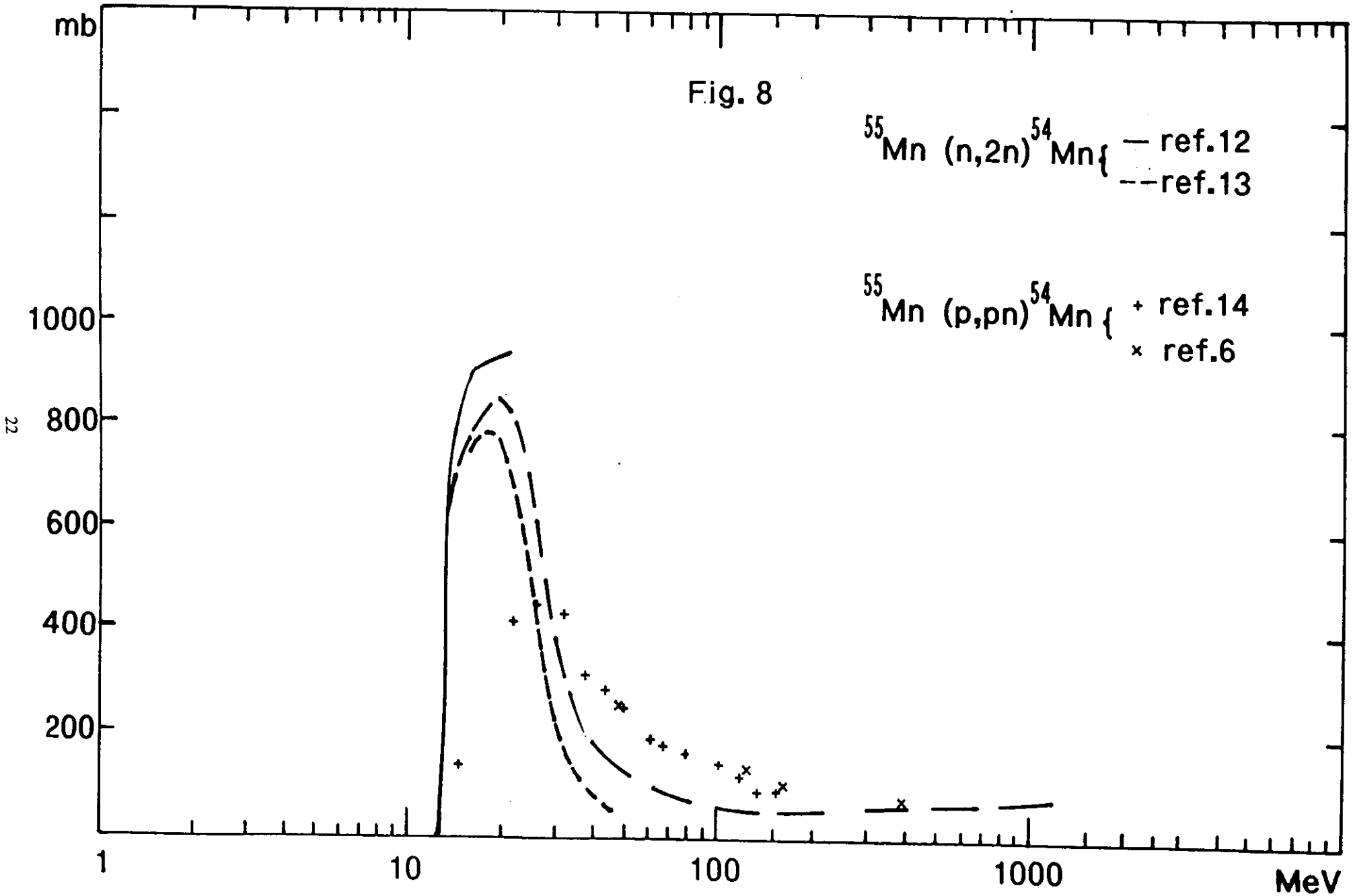
mb
Fig. 8
^{55}Mn (n,2n)^{54}Mn
ref.12
ref.13
^{55}Mn (p,pn)^{54}Mn
ref.14
ref.6
1000
800
600
400
200
1
10
100
1000
MeV

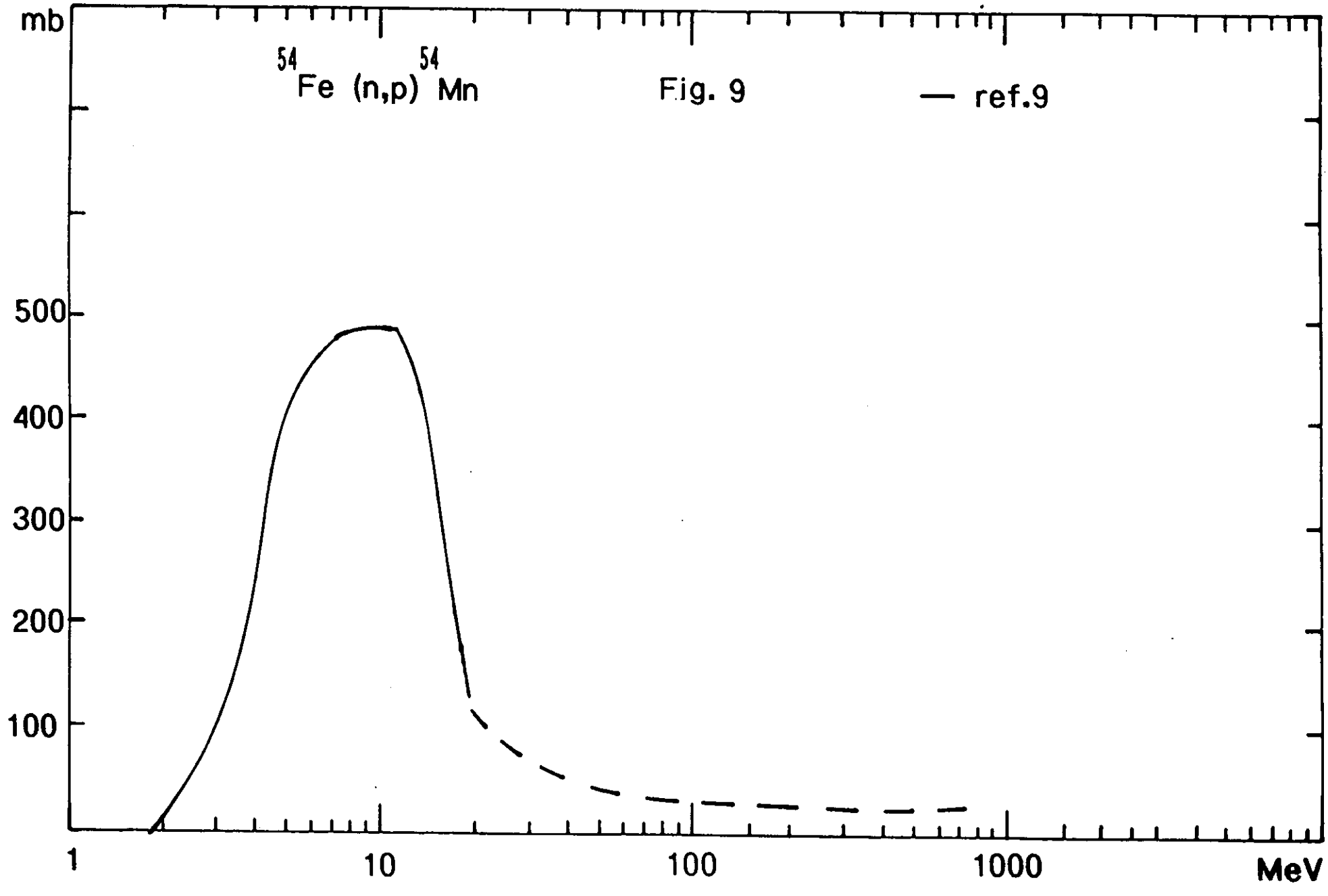
mb
54 54
Fe (n,p) Mn
Fig. 9
— ref.9
500
400
300
200
100
1
10
100
1000
MeV

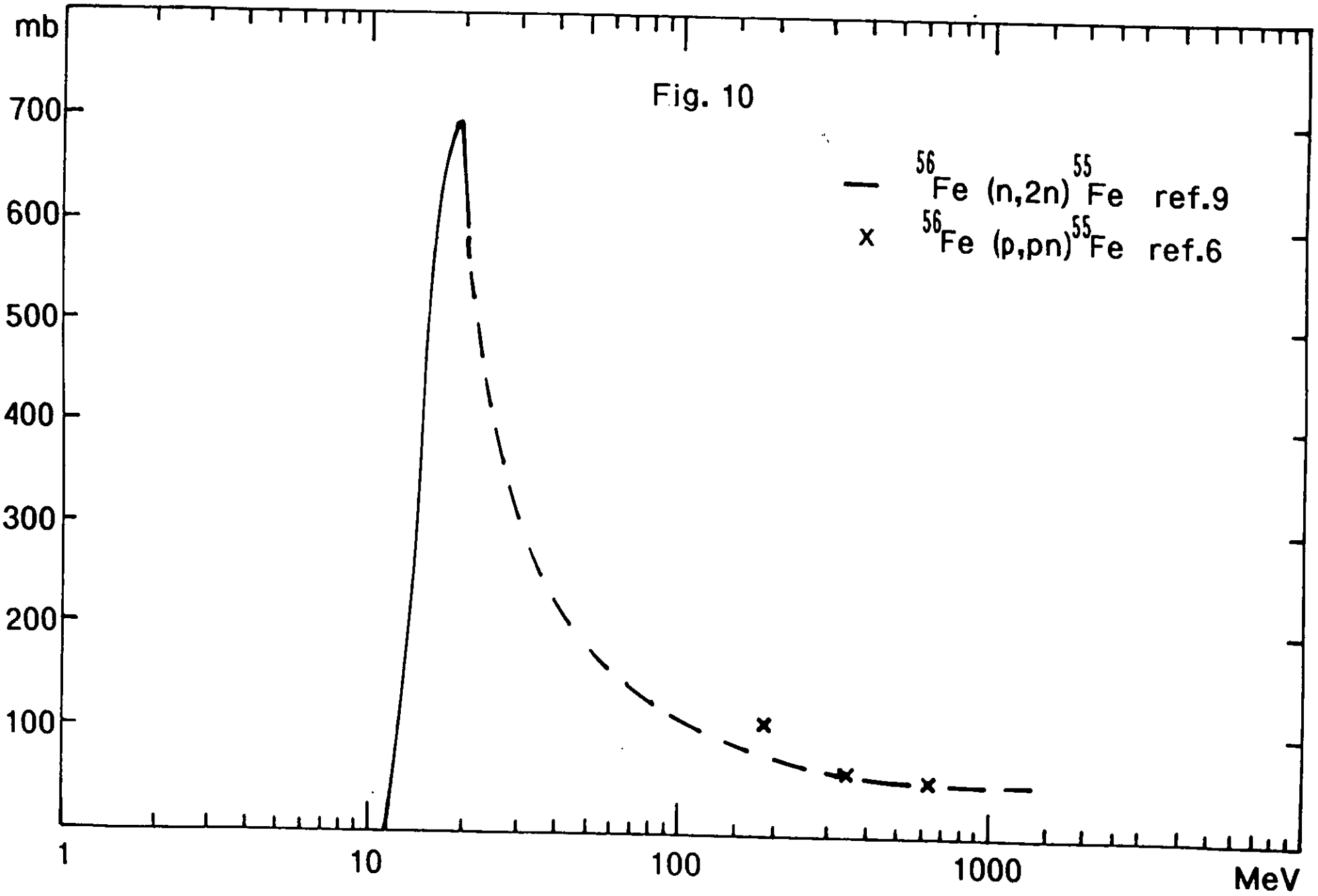
mb
700
600
500
400
300
200
100
1
10
100
1000
MeV
— ^{56}Fe (n,2n)^{55}Fe ref.9
x ^{56}Fe (p,pn)^{55}Fe ref.6

Fig. 10

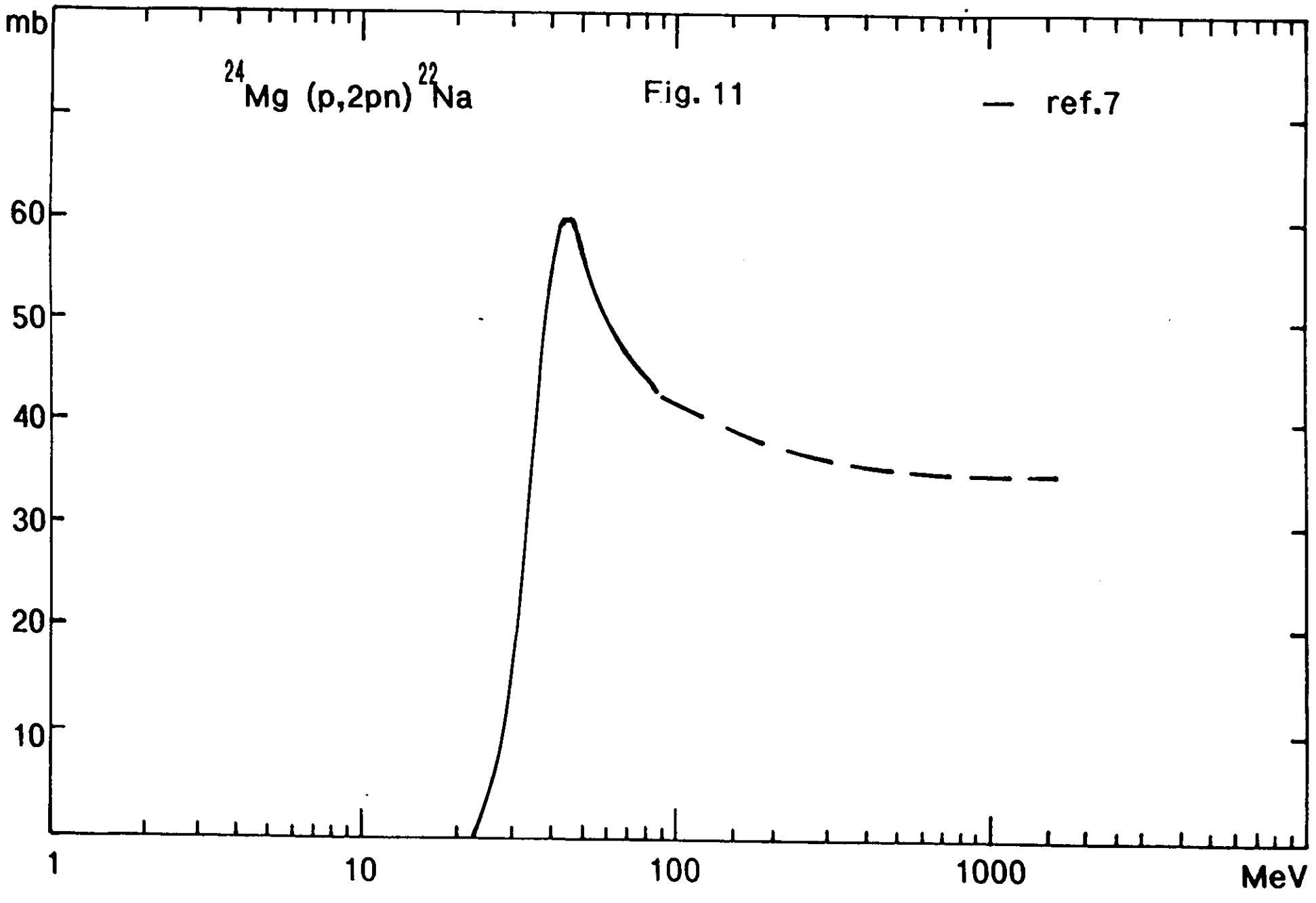
mb
^{24}Mg (p,2pn) ^{22}Na
Fig. 11
— ref.7
60
50
40
30
20
10
1
10
100
1000
MeV